



Room-temperature multiferroic behavior in layer-structured Aurivillius phase ceramics

Cite as: Appl. Phys. Lett. **117**, 052903 (2020); <https://doi.org/10.1063/5.0017781>

Submitted: 09 June 2020 . Accepted: 25 July 2020 . Published Online: 07 August 2020

Zheng Li, Vladimir Koval , Amit Mahajan, Zhipeng Gao, Carlo Vecchini, Mark Stewart, Markys G. Cain , Kun Tao, Chenglong Jia , Giuseppe Viola, and Haixue Yan 



View Online



Export Citation



CrossMark

ARTICLES YOU MAY BE INTERESTED IN

[Intrinsic piezoelectricity in \(K,Na\)NbO₃-based lead-free single crystal: Piezoelectric anisotropy and its evolution with temperature](#)

Applied Physics Letters **117**, 052904 (2020); <https://doi.org/10.1063/5.0012124>

[Current-induced bulk magnetization of a chiral crystal CrNb₃S₆](#)

Applied Physics Letters **117**, 052408 (2020); <https://doi.org/10.1063/5.0017882>

[Magnetic transition behavior and large topological Hall effect in hexagonal Mn_{2-x}Fe_{1+x}Sn \(x = 0.1\) magnet](#)

Applied Physics Letters **117**, 052407 (2020); <https://doi.org/10.1063/5.0011570>



Measure Ready
FastHall™ Station

The highest performance tabletop system

[Learn more](#)

Lake Shore
CRYOTRONICS

Room-temperature multiferroic behavior in layer-structured Aurivillius phase ceramics

Cite as: Appl. Phys. Lett. 117, 052903 (2020); doi: 10.1063/5.0017781

Submitted: 9 June 2020 · Accepted: 25 July 2020 ·

Published Online: 7 August 2020 · Corrected: 11 August 2020



Zheng Li,¹ Vladimir Koval,² Amit Mahajan,³ Zhipeng Gao,⁴ Carlo Vecchini,⁵ Mark Stewart,⁵ Markys G. Cain,⁶ Kun Tao,⁷ Chenglong Jia,^{7,a)} Giuseppe Viola,³ and Haixue Yan^{3,b)}

AFFILIATIONS

¹Guangdong Provincial Key Laboratory of Applied Superconductivity, Institute of Superconducting Ceramics, Guangdong Academy of Sciences, Guangzhou 510650, China
²Institute of Applied Physics, Faculty of Science, Beijing University of Aeronautics and Astronautics, Beijing 100191, China
³Department of Applied Physics, Faculty of Science, Beijing University of Aeronautics and Astronautics, Beijing 100191, China
⁴National Key Laboratory of Applied Superconductivity, Institute of Superconducting Ceramics, Guangdong Academy of Sciences, Guangzhou 510650, China
⁵Department of Applied Physics, Faculty of Science, Beijing University of Aeronautics and Astronautics, Beijing 100191, China
⁶Department of Applied Physics, Faculty of Science, Beijing University of Aeronautics and Astronautics, Beijing 100191, China
⁷Department of Applied Physics, Faculty of Science, Beijing University of Aeronautics and Astronautics, Beijing 100191, China

a)Email: chenglong.jia@buaa.edu.cn
 b)Author to whom correspondence should be addressed: yanhx@buaa.edu.cn

ABSTRACT

Room-temperature multiferroic behavior is reported in layer-structured Aurivillius phase ceramics (Bi_{5.25}La_{0.75}F₂C₁₂O₁₈) with the general formula of Bi_{5-2x}L_xF₂C₁₂O₁₈ (x = 0.25, 0.5, 0.75). The structural and magnetic properties are investigated by X-ray diffraction, Raman spectroscopy, and *in situ* neutron diffraction. The results show that the Aurivillius phase ceramics exhibit a magnetic transition at room temperature, which is attributed to the presence of the B³⁺ O F³⁺, C³⁺ O C³⁺, and F³⁺ O C³⁺ groups. The magnetic transition is associated with the A²⁺ B²⁺ O₃ group, which is a characteristic feature of the Aurivillius phase. The magnetic transition is observed in the Aurivillius phase ceramics with the general formula of Bi_{5-2x}L_xF₂C₁₂O₁₈ (x = 0.25, 0.5, 0.75). The magnetic transition is associated with the A²⁺ B²⁺ O₃ group, which is a characteristic feature of the Aurivillius phase. The magnetic transition is observed in the Aurivillius phase ceramics with the general formula of Bi_{5-2x}L_xF₂C₁₂O₁₈ (x = 0.25, 0.5, 0.75).

Published under license by AIP Publishing. <https://doi.org/10.1063/5.0017781>

Multiferroic (FM) (FE) Aurivillius phase ceramics (B₅F₂C₁₂O₁₈) (= 4) (B₆F₂C₁₂O₁₈) (= 5), (B₄F₂C₁₂O₁₈) (= 3) (B_{5.25}F₂C₁₂O₁₈) (= 3.75) (B_{4.5}F₂C₁₂O₁₈) (= 3.5) (B_{3.75}F₂C₁₂O₁₈) (= 3.25) (B₃F₂C₁₂O₁₈) (= 3) (B_{2.25}F₂C₁₂O₁₈) (= 2.75) (B_{1.5}F₂C₁₂O₁₈) (= 2) (B_{0.75}F₂C₁₂O₁₈) (= 1.5). The magnetic transition is observed in the Aurivillius phase ceramics with the general formula of Bi_{5-2x}L_xF₂C₁₂O₁₈ (x = 0.25, 0.5, 0.75). The magnetic transition is associated with the A²⁺ B²⁺ O₃ group, which is a characteristic feature of the Aurivillius phase. The magnetic transition is observed in the Aurivillius phase ceramics with the general formula of Bi_{5-2x}L_xF₂C₁₂O₁₈ (x = 0.25, 0.5, 0.75).

$B_{5.25}L_{0.75}F_3C_{3O_{18}}$
 (BLFC) P L A P C, D
 $a b$ P
 BLFC
 $a b$ A
 18
 A, *in situ* I H I I
 N, AL, D, O, U K.
 F
 (P). A BLFC
 P
 BLFC P.
 F 1 (D) BLFC
 A
 $B2cb$ A
 A, $19,20$ A_{21}
 $B2cb$ $a = 5.4530(2)$ A, $b = 5.4427(1)$ A,
 $c = 50.670(2)$ A $A_{21}am$ $a = 5.4651(6)$ A,
 $b = 5.3943(6)$ A, $c = 41.487(2)$ A
 F P (//

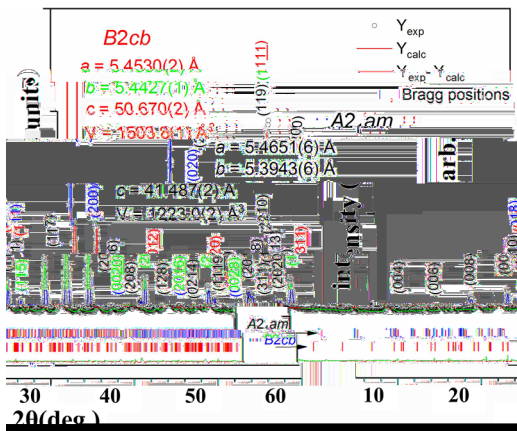


FIG. 1. XRD pattern of B2cb and A2,am phases.

BLFC = 4 = 5 A . N
 BLFC F 1 EM (a-b) D
 P M
 F . 1 1.4 %, (F . 2
 D. ED
 1)
 F, C, O, C₂F₂O₄
 A B₅F_{0.5}C_{0.5}O₁₅.¹⁶
 BLFC (50, 70 100,
 300, 500 H).
 1060 K FE T BLFC . H , B₆F₃O₁₈
 (973 K).¹³ F 2() P-E I-E
 BLFC P I-E
 $21,22$
 BLFC $10 \mu C / ^2$.
 F 2() (FC)
 200 O BLFC BLFC

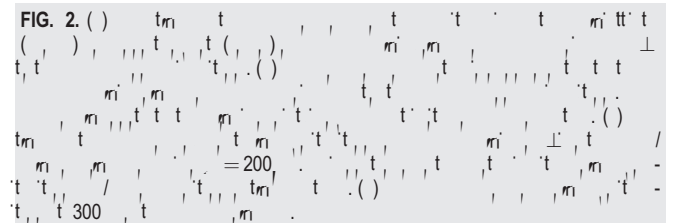
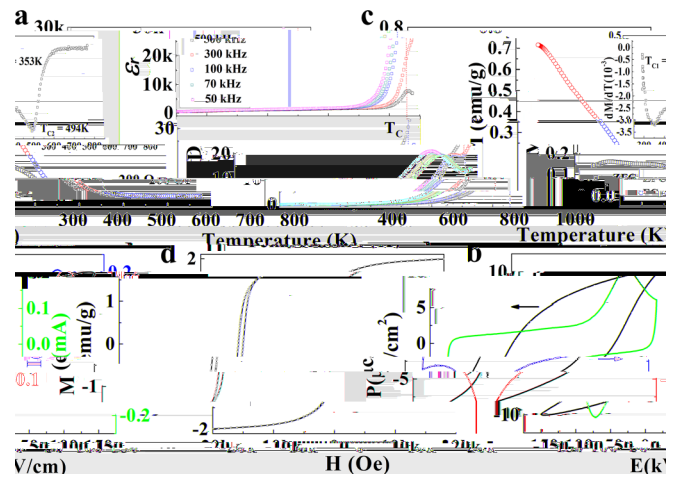


FIG. 2. (a) Temperature dependence of dielectric loss (ε'') for BLFC at frequencies of 300 kHz, 100 kHz, 70 kHz, and 50 kHz. (b) Temperature dependence of the real part of the dielectric function (ε'). (c) Temperature dependence of the imaginary part of the dielectric function (ε''). (d) Temperature dependence of the piezoelectric coefficient (P) in units of μC/cm². (e) Temperature dependence of the piezoelectric coefficient (P) in units of μC/cm². (f) Temperature dependence of the piezoelectric coefficient (P) in units of μC/cm². (g) Temperature dependence of the piezoelectric coefficient (P) in units of μC/cm². (h) Temperature dependence of the piezoelectric coefficient (P) in units of μC/cm². (i) Temperature dependence of the piezoelectric coefficient (P) in units of μC/cm².

~ 494 K
 $M/$),
 $B_6F C_3O_{18}$ (526 K).²³
 BLFC
 $F^{3+} O F^{3+}, C^{3+} O C^{3+}, F^{3+} O C^{3+}$ (.
 ED
 FC $2 \sim 353$ K
 $C_2F O_4$ 2 $16,25$
 $C_2F O_4$ (460 K)
 $(M) C_2F O_4$ 1.4 . %
 $16 \ 23.5 / .^{25}$, 0.22 0.32 / ,
 $C_{2-} F O_4$ BLFC
 $M = 1.85 / , F . 2() . I$, M H
 $2 (F . 3)$ 1
 425 K 1.58 / . 0.27 / , ED
 BLFC
 A
 $F 3$
 $F^{3+} O C^{3+}$ *ab initio*
 (DF) H
 $(A P)$ C
 $U_F = 2$ $U_C = 3$ F C ,
 $(GGA)U$. I
 BLFC
 $F . 3() , F^{3+} C^{3+} (3.1 \ 2.1 \mu_B/ ,)$,
 O
 $(0.1 \ \mu_B/)$.
 $F O_6$ $C O_6$ F / C -
 F O - / $F . 3()$.
 $F^{3+} C^{3+}$,
 $(. ,)$ (. ,)
 $E_{FM} - E_{AFM}$
 $= -144.1$.
 H , (FM)
 43.5 (. , 504.6 K), FM
 1 FC/FC $F . 2()$ 2 ,
 $a b$,
 010 .
 BLFC $F 4$. I
 399 O .
 $F .$
 P F M
 $5() . A$ PFM BLFC ,
 $F -$

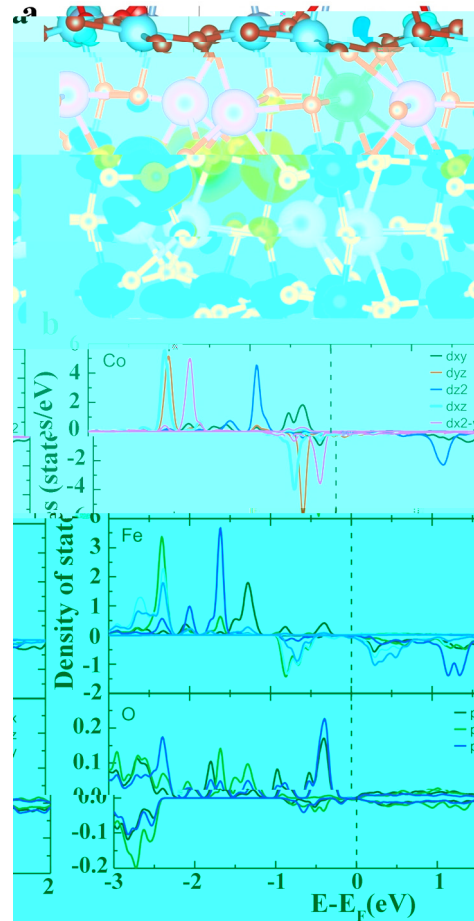


FIG. 3. (a) Crystal structure of BLFC. (b) Density of states (DOS) for Co, Fe, and O atoms. The DOS is calculated using the GGA+U method with $U_F = 2$ eV and $U_C = 3$ eV. The x-axis is the energy relative to the Fermi level ($E - E_F$) in eV, and the y-axis is the density of states in states/eV. The legend indicates the contributions from different orbitals: dxy (green), dyz (red), dz2 (blue), dxz (cyan), and dx2-y2 (magenta).

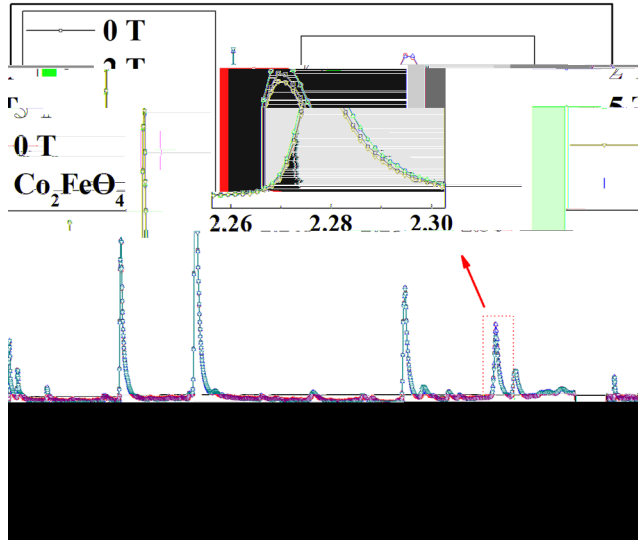


FIG. 4. XRD patterns of BLFC film on Co₂FeO₄ substrate. The inset shows the schematic of the BLFC film on the Co₂FeO₄ substrate. The XRD patterns show peaks at 2.26, 2.28, and 2.30 nm. A red arrow points to a peak at 2.30 nm.

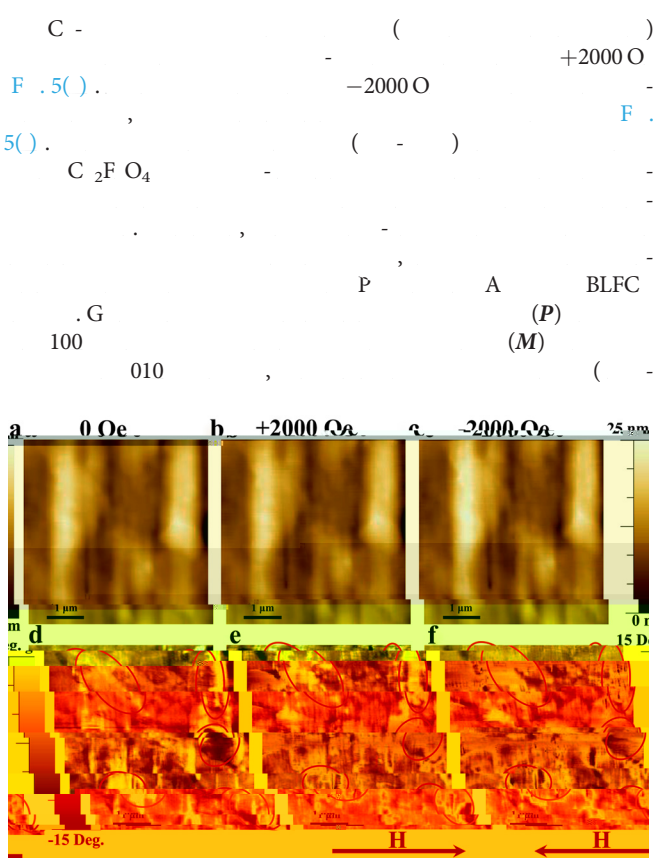


FIG. 5. MFM images of BLFC film at different magnetic fields. (a) 0 Oe, (b) +2000 Oe, (c) -2000 Oe. The images show the magnetic domain structure of the BLFC film. The scale bar is 25 nm. The images are labeled with 'a', 'b', 'c' and 'd', 'e', 'f'.

$T = P \times M$
 BLFC
 I , A BLFC
 F
 $C^{3+} O C^{3+}, F^{3+} O C^{3+}$
 $F^{3+} O F^{3+}$
 A , C / F
 EM (ED)
 BLFC
 D . M , P D . K , D.
 D I H I I N , AL,
 D , O K.
 A E D F
 G A A (G N . 2/
 0038/20), C (G N . K2015-0602006), N FC (G
 N . 11474138 11834005). A
 E M P (EM P)
 P IND54 N EM P
 EM P E PAME E

DATA AVAILABILITY

REFERENCES

1. E , N. D. M , J. F. , N 442, 759 (2006).
2. N. A. , N . M . 6, 21 (2007).
3. J. M. , J. H. , L. C. . N , A . M . 23, 1062 (2011).
4. L. F. H , O. C , J. B , J. L , C. H , H , O. G , D. C. L , H. , K , A. J. B , A . F . M . 26, 2111 (2016).
5. N. A. H , J. P . C . B 104, 6694 (2000).
6. B. A , M : IL
 B₄O₁₂, A . K 1(58), 499-512 (1949).
7. A. , G. K , M. M. K , J. P . C . M . 11, 3335 (1999).
8. N. . P G. . K , M . . E . B 108, 194 (2004).
9. L. K , M , M. , A. A , N. D , N. P , M. E. P , D. J , J. A . C . . 96, 2339 (2013).
10. L. J. M , G , G. , K , A. M , L. C. J , C. N , H. , D . 45, 14049 (2016).
11. J. F. , NPGA M . 5, 72 (2013).
12. A. B C. E , P . B 90, 214109 (2014).
13. J. B. L. , P. H , G. H , G. . L , J. L , J. C , J. K. L , A . P . L . 96, 222903 (2010).
14. M , . C , . L , A . P . L . 95, 082901 (2009).
15. L. J. , L. , J. D , A . P . L . 101, 122402 (2012).

- ¹⁶M. P. , P. C. , M. B. , A. P. B. , J. P. H. , K. , L. K. , M. P. , C. , H. K. , A. J. B. , *J. A. P.* **112**, 073919 (2012).
- ¹⁷J. L. , H. , M. J. , K. , P. , *J. A. P.* **102**, 104107 (2007).
- ¹⁸M. G. C. , *Characterisation of Ferroelectric Bulk Materials and Thin Films* (, 2014), .2.
- ¹⁹.L., K. , J. M. , .G. , .K. , C. J. , G. , H. , A. M. , J. C. , M. C. , I. A. , C. N. , C. J. , H. , *J. M. C. C* **6**, 2733 (2018).
- ²⁰.K. , I. , G. , M. , C. J. , H. , *J. P. C.* **122**, 15733 (2018).
- ²¹L. J. , F. L. , , *J. A. C.* **97**, 1 (2014).
- ²²H. , F. I. , G. , H. N. , H. , J. , .G. , M. J. , *J. A. D.* **1**, 107 (2011).
- ²³J. , L. , .L. , . , J. D. , , A. . *P. L.* **101**, 012402 (2012).
- ²⁴B. , J. , J. C. , .L. , . , J. D. , , . , *A. P. L.* **104**, 062413 (2014).
- ²⁵I. P. M. , N. B. , . . **11**, 719 (2009).